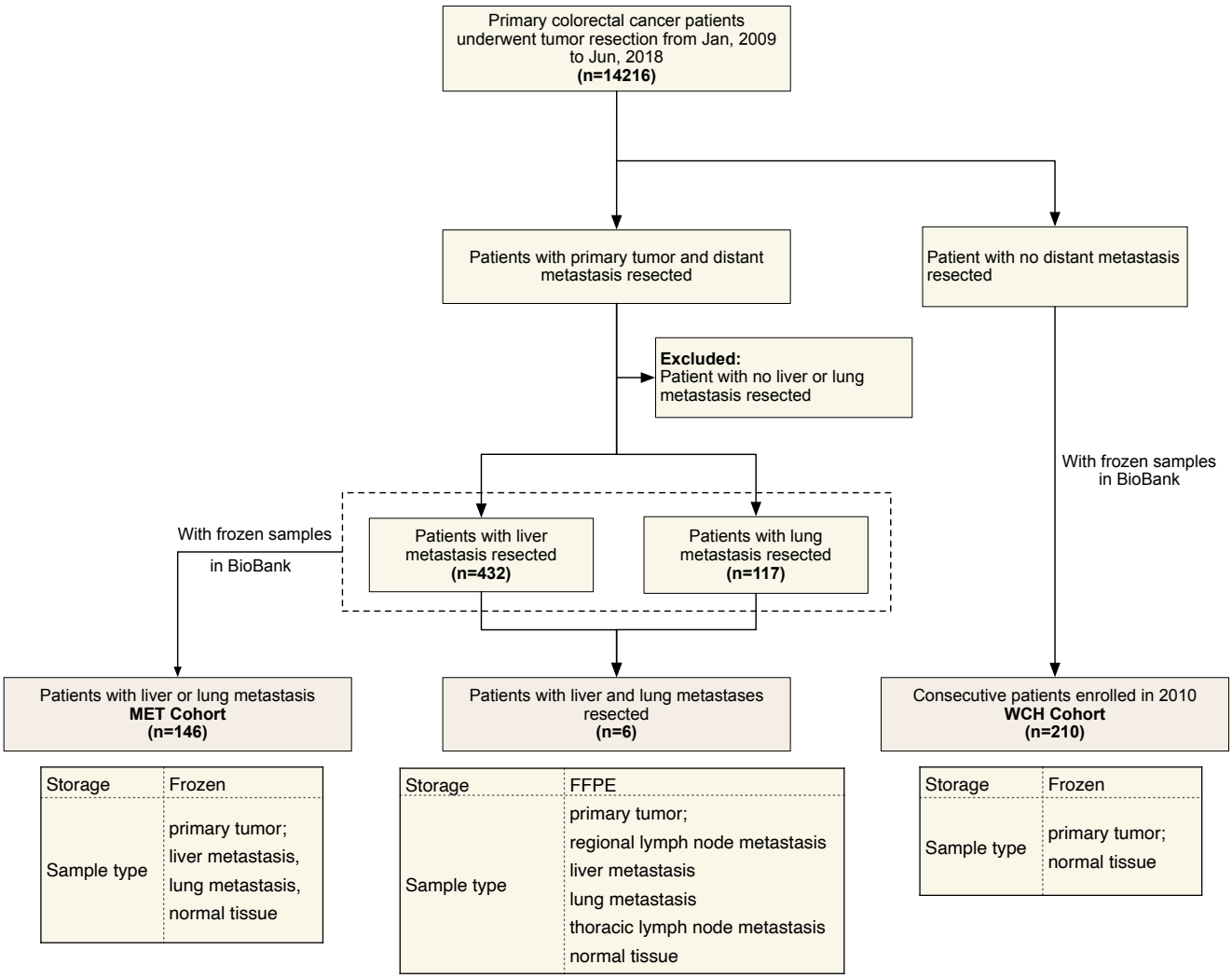

Figure S1. Study flowchart. Related to Figure 1 and Figure 6
Diagram for patient selection in this study. FFPE, formalin-fixed paraffin-embedded.

A

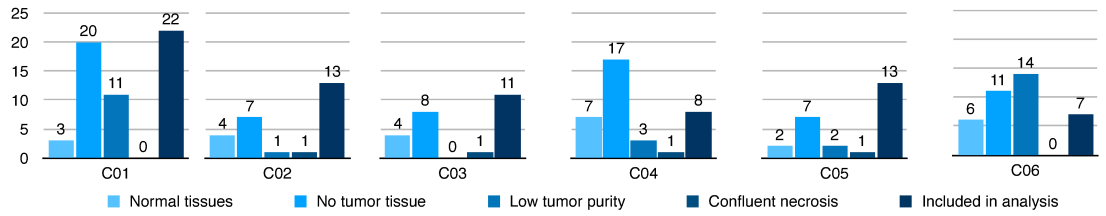

B

	C01	C02	C03	C04	C05	C06
NOM	1 (4)	1 (5)	1 (5)	1 (8)	1 (3)	1 (7)
PRM	5 (9)	3 (3)	3 (3)	3 (5)	3 (4)	1 (10)
RLN	3 (7)	2 (10)	0 (4)	0 (16)	0 (2)	0 (9)
LIM	4 (4)	3 (4)	3 (4)	3 (4)	6 (7)	3 (4)
LUM	6 (13)	4 (4)	4 (4)	1 (2)	3 (4)	2 (3)
TLN	3 (19)	0 (0)	0 (4)	0 (1)	0 (5)	0 (5)
Total	22 (56)	13 (26)	11 (24)	8 (36)	13 (25)	7 (38)

C

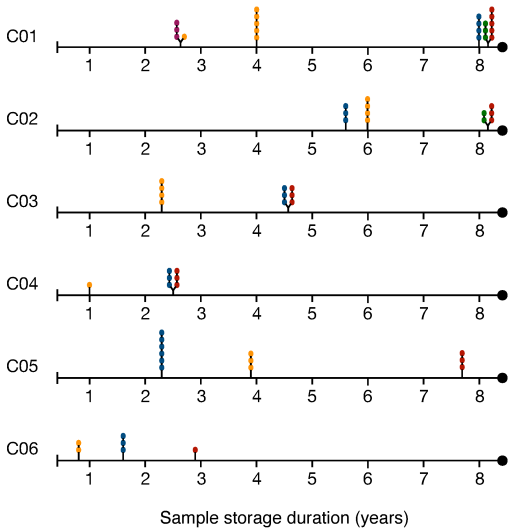

Figure S2. Sample selection from included patients. Related to Figure 1
(**A**) A total of 205 formalin-fixed paraffin-embedded (FFPE) tissue blocks were collected from the included six patients. Tumor purity and tissue quality were estimated based on histological sections of each sample by a pathologist. Samples with low tumor purity or confluent necrosis were excluded. (**B**) In total, 74 patient-matched samples were obtained for subsequent analysis and sample contributions from each case were summarized. Digital slides of included samples were obtained using Pannoramic MIDI (3DHISTECH Ltd) and were reported in **Data S1.** (**C**) The storage durations of samples in each patient were demonstrated. Abbreviations: NOM, normal colon/rectum tissue; PRM, primary colorectal cancer; RLN, regional lymph node metastasis; LIM, liver metastasis; LUM, lung metastasis; TLN, thoracic lymph node metastasis.

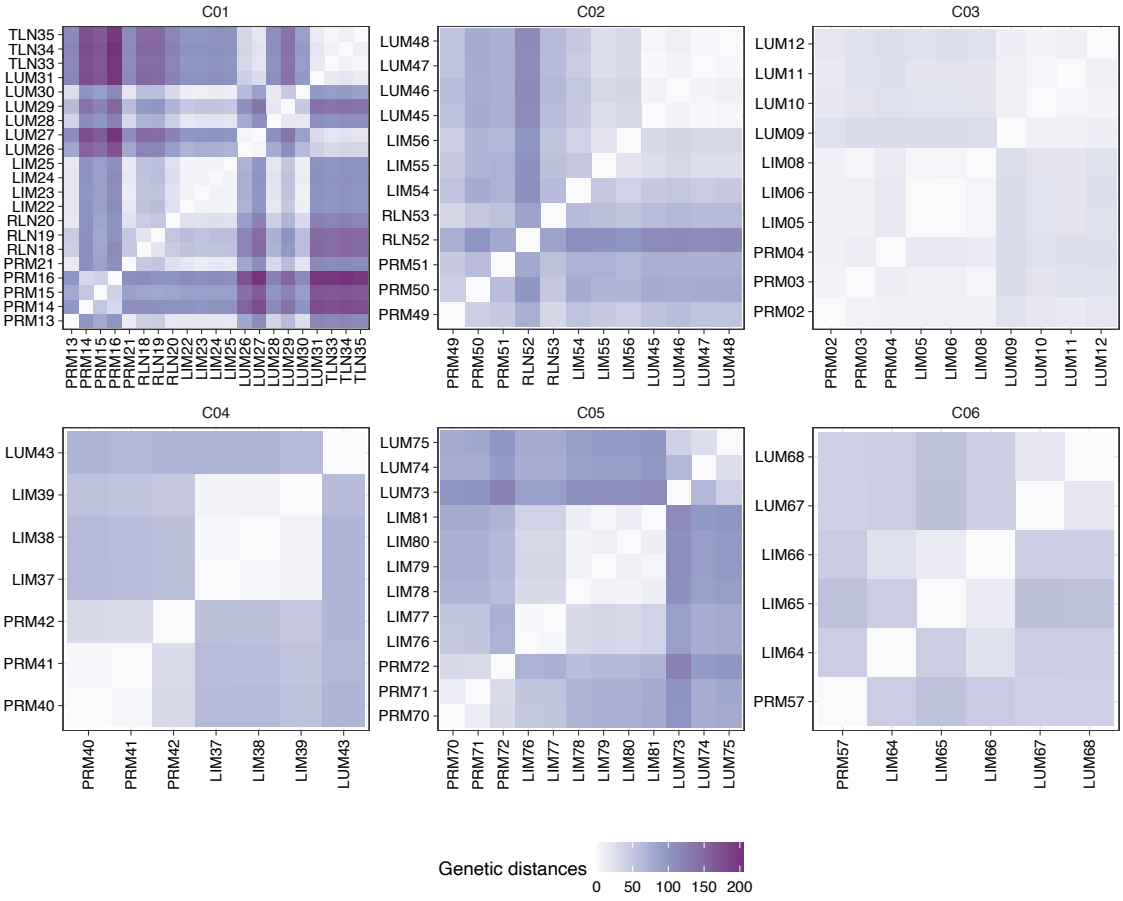

Figure S3. Pairwise genetic distances among tumor samples in each patient. Related to Figure 1

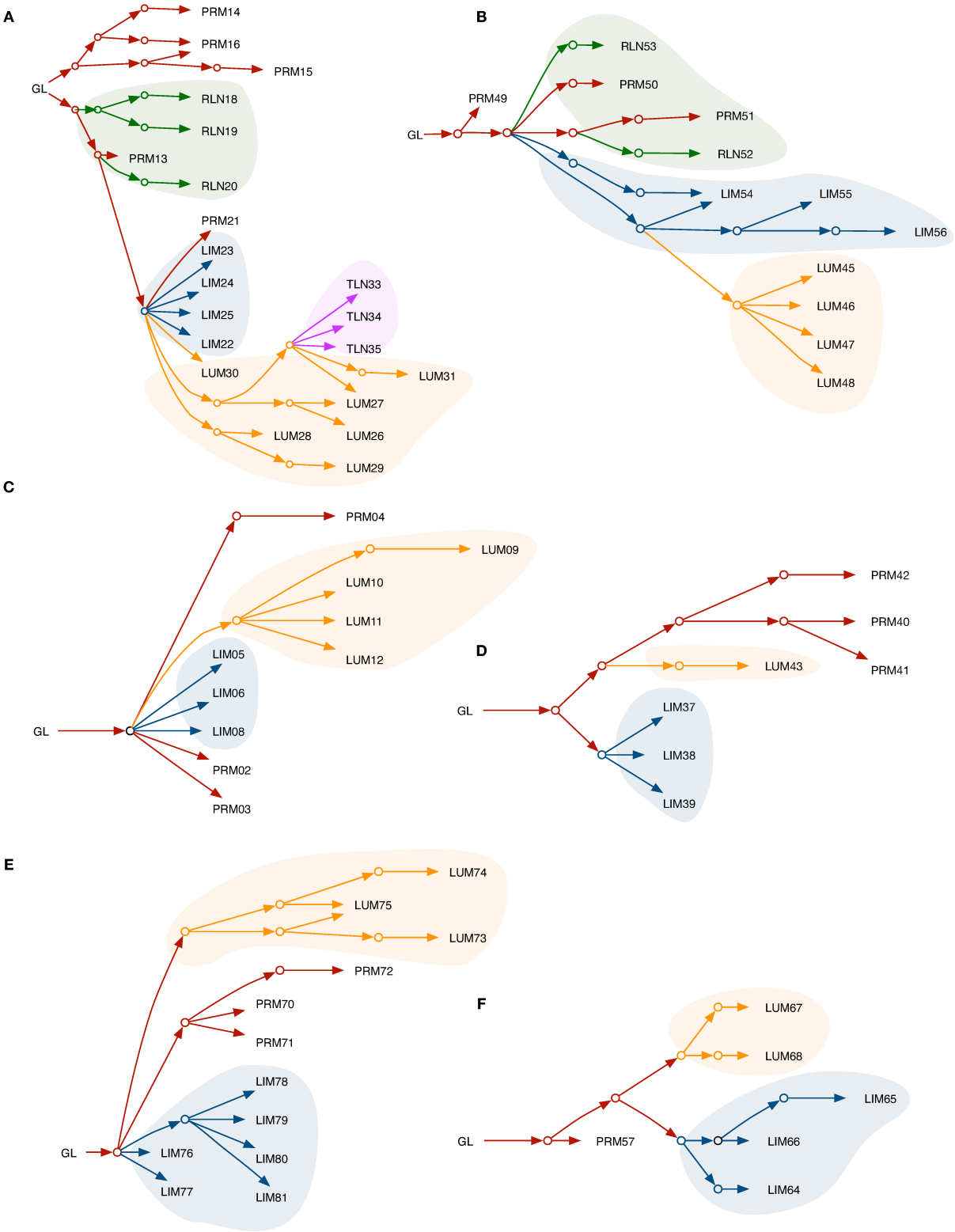

Figure S4. Inference of colorectal cancer metastasis lineages using LICHeE. Related to Figure 2
Phylogenetic analysis of the relationships of the primary tumor to the regional/distant metastases in patients C01 (**A**), C02 (**B**), C03 (**C**), C04 (**D**), C05 (**E**), and C06 (**F**) using LICHeE. Abbreviations: PRM, primary colorectal cancer; RLN, regional lymph node metastasis; LIM, liver metastasis; LUM, lung metastasis; TLN, thoracic lymph node metastasis.

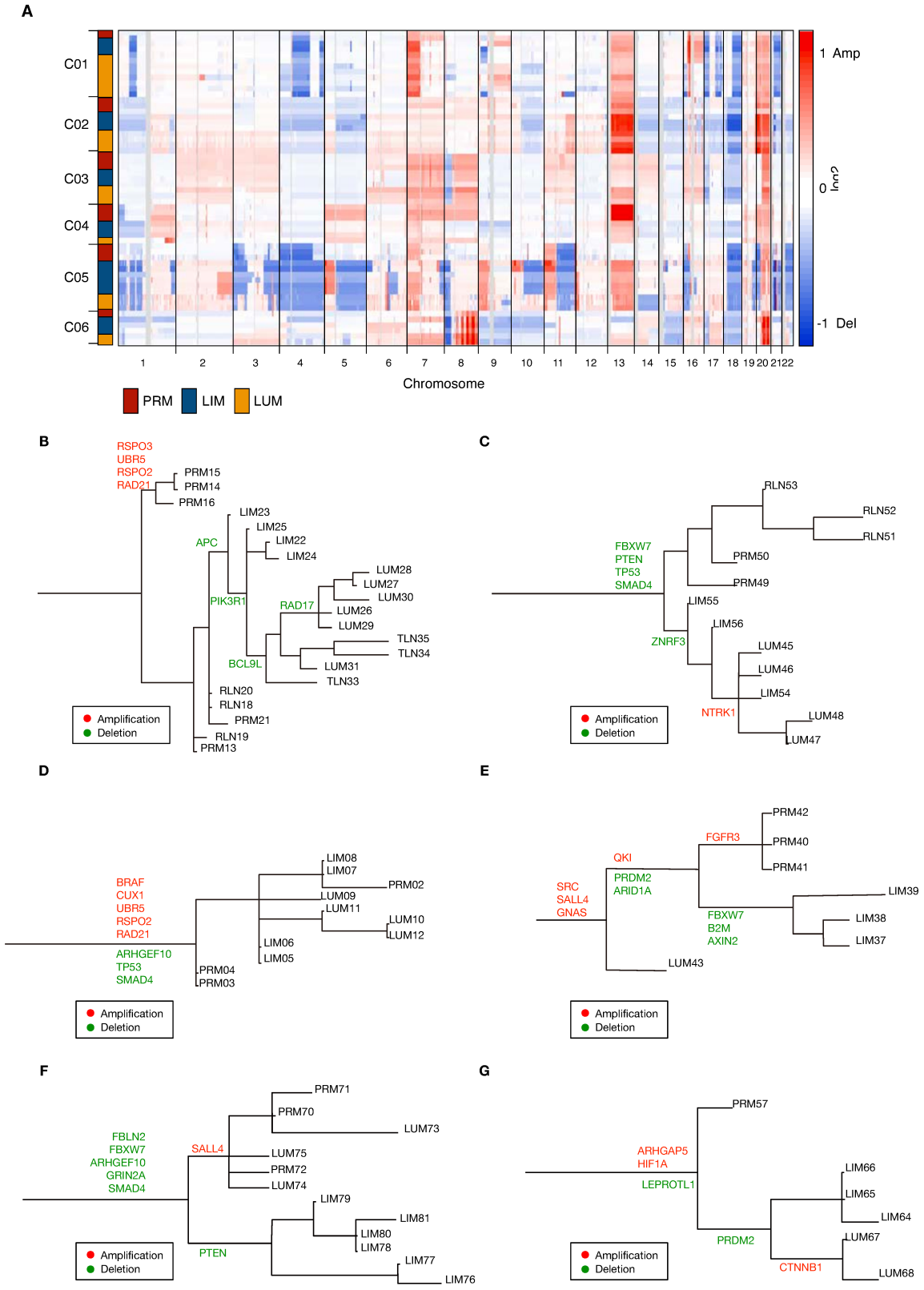

Figure S5. Exome-sequencing-based copy number alterations. Related to Figure 2 and 3.
(**A**) Exome-sequencing-based copy number alterations in each chromosome.The phylogenetic trees were reconstructed based on the alterations of copy number across all samples for patient C01(**B**), C02(**C**), C03(**D**), C04(**E**), C05(**F**), and C06(**G**) using a Minimum Event Distance for Intra-tumor Copy-number Comparisons (MEDICC) algorithm. Abbreviations: PRM, primary colorectal cancer; RLN, regional lymph node metastasis; LIM, liver metastasis; LUM, lung metastasis; TLN, thoracic lymph node metastasis.

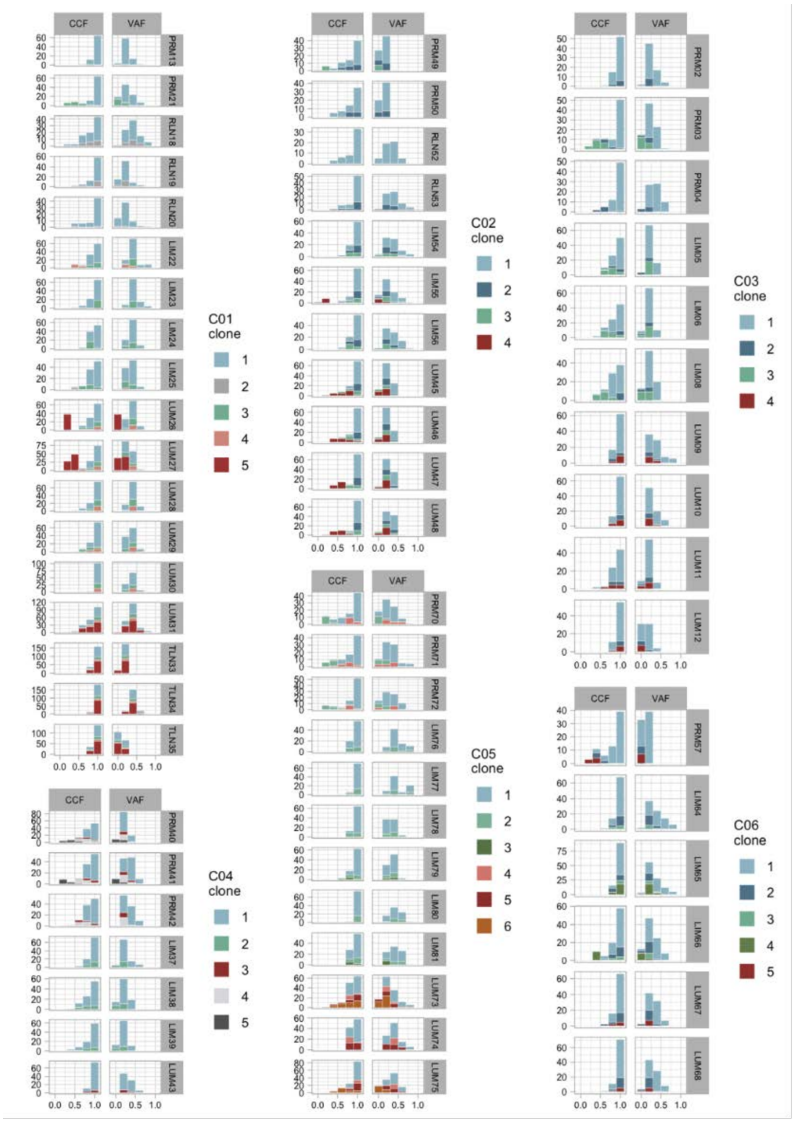

Figure S6. The unadjusted VAF and CCF histogram for each sample in patient C01-06 with clone annotated. Related to Figure 3.

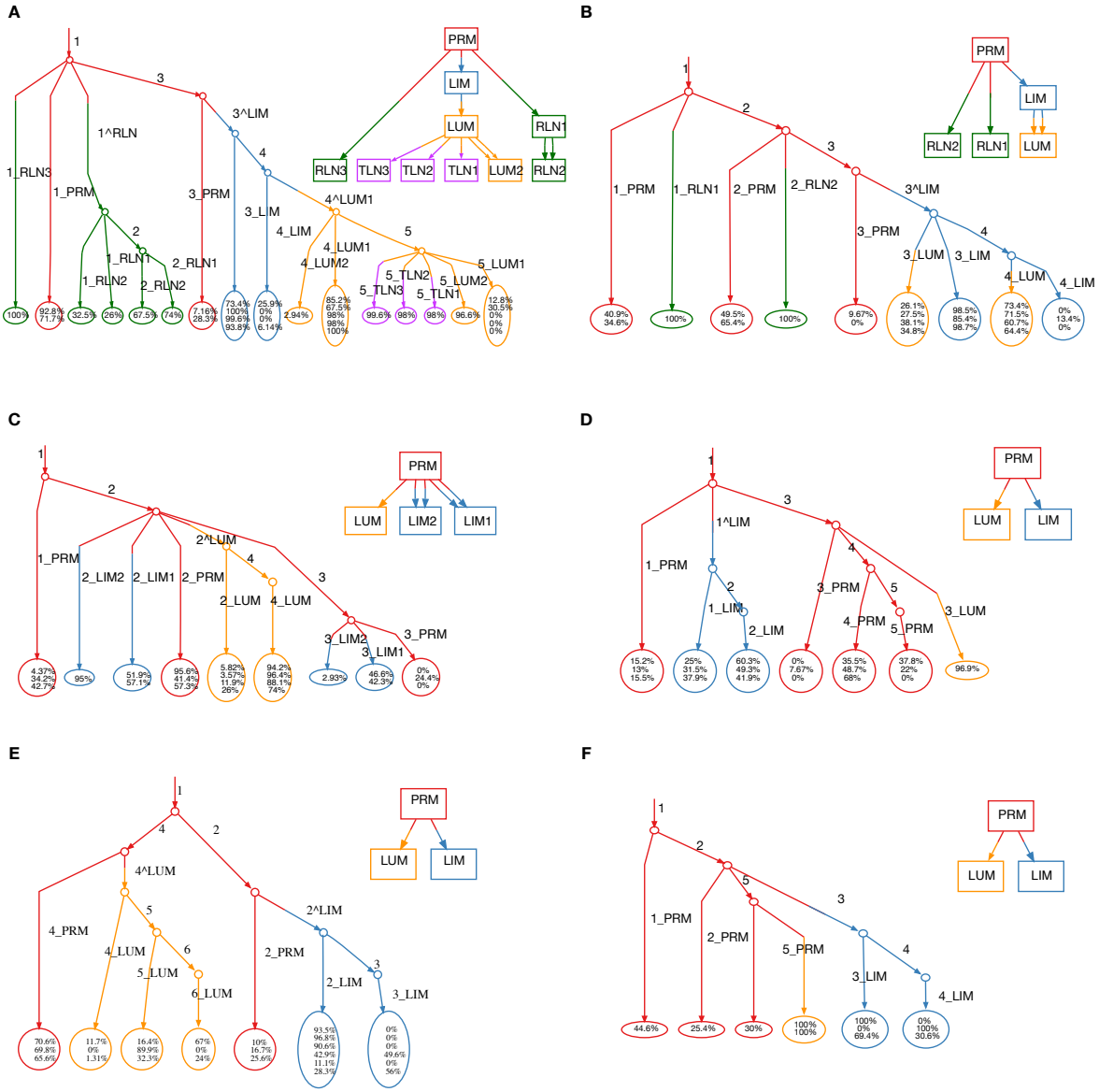

Figure S7. Inferring migration histories for metastatic colorectal cancers using MACHINA. Related to Figure 2 and 3
Phylogenetic analysis of the relationships of the primary tumor to the regional/distant metastases in patients C01 (**A**), C02 (**B**), C03 (**C**), C04 (**D**), C05 (**E**), and C06 (**F**) using MACHINA. Abbreviations: PRM, primary colorectal cancer; RLN, regional lymph node metastasis; LIM, liver metastasis; LUM, lung metastasis; TLN, thoracic lymph node metastasis.

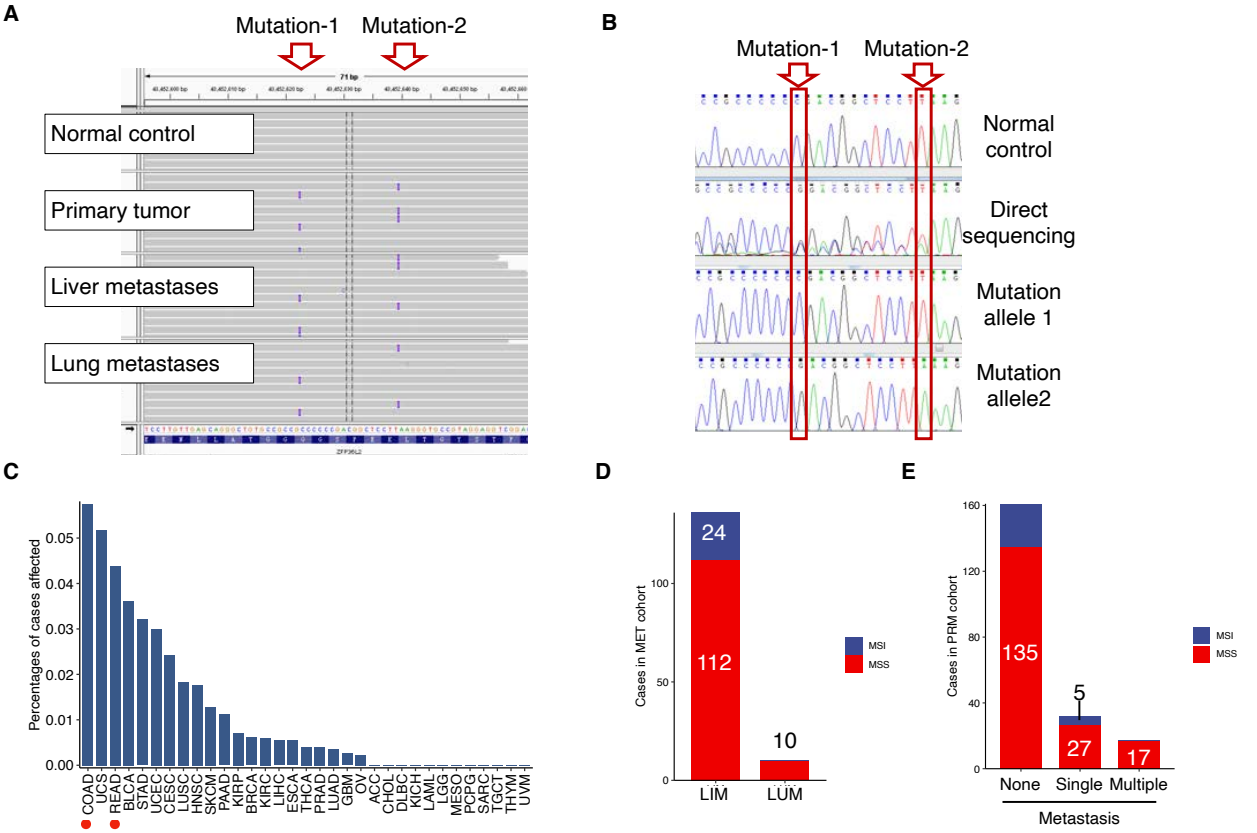

Figure S8. illustration of compound heterozygous mutations of *ZFP36L2* in patient C03. Related to Figure 6.
(**A**) Two frameshift mutations of *ZFP36L2* were illustrated with IGV software in normal control, primary colorectal cancer, liver metastases and lung metastases, respectively. (**B**) Validation with Sanger sequencing in normal tissue and primary tumor (upper two trace). Each mutation was separately genotyped after single clone selection with T-vector (lower two traces). (**C**) Somatic mutations data of ZFP36L2 for all cancer types were obtained from the Cancer Genome Atlas. Only non-silent variants (missense mutations, nonsense mutations, nonstop mutations, frameshift insertion/deletions, and splice site mutations) were considered to illustrate the mutation frequencies across different cancer types. ZFP36L2 mutations were enriched in COAD and READ cohorts, namely colorectal cancers. (**D**) Sample characteristic in MET cohort. (**E**) Sample characteristic in PRM cohort.

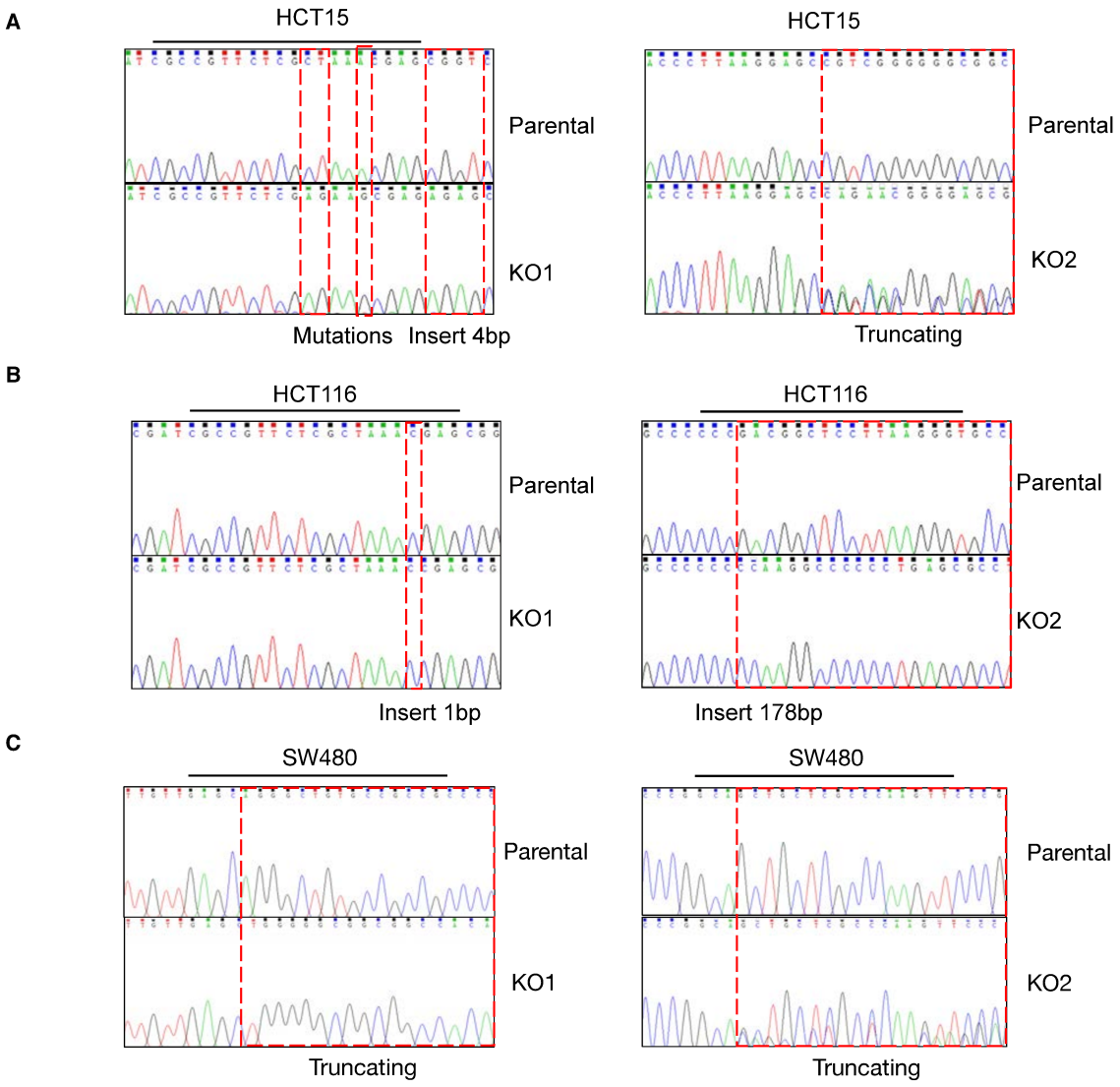

Figure S9. Sanger sequencing in parental and *ZFP36L2*-KO CRC cells. Related to Figure 6.
(**A**) Sanger sequencing in HCT15-parental and HCT15-KO cells. (**B**) Sanger sequencing in HCT116-parental and HCT116-KO cells. (**C**) Sanger sequencing in SW480-parental and SW480-KO cells. KO, *ZFP36L2* knock-out clone.